Journal of Power Sources 195 (2010) 3546–3552

Contents lists available at ScienceDirect

Journal of Power Sources

journal homepage: www.elsevier.com/locate/jpowsour

Corrosion resistance characteristics of stamped and hydroformed proton exchange membrane fuel cell metallic bipolar plates

F. Dundar[a,b], Ender Dur[a], S. Mahabunphachai[a,c], M. Koç[a,*]

[a] NSF I/UCRC Center for Precision Forming (CPF), Virginia Commonwealth University, Richmond, VA, USA
[b] Department of Materials Science and Engineering, Gebze Institute of Technology, Turkey
[c] National Metal and Materials Technology Center (MTEC), Pathumthani, Thailand

ARTICLE INFO

Article history:
Received 31 October 2009
Received in revised form 9 December 2009
Accepted 10 December 2009
Available online 4 January 2010

Keywords:
Metallic bipolar plates
PEMFC
Corrosion
Micro-manufacturing
Micro-channels
Hydroforming
Stamping

ABSTRACT

Metallic bipolar plates have several advantages over bipolar plates made from graphite and composites due to their high conductivity, low material and production costs. Moreover, thin bipolar plates are possible with metallic alloys, and hence low fuel cell stack volume and mass are. Among existing fabrication methods for metallic bipolar plates, stamping and hydroforming are seen as prominent approaches for mass production scales. In this study, the effects of important process parameters of these manufacturing processes on the corrosion resistance of metallic bipolar plates made of SS304 were investigated. Specifically, the effects of punch speed, pressure rate, stamping force and hydroforming pressure were studied as they were considered to inevitably affect the bipolar plate micro-channel dimensions, surface topography, and hence the corrosion resistance. Corrosion resistance under real fuel cell conditions was examined using both potentiodynamic and potentiostatic experiments. The majority of the results exhibited a reduction in the corrosion resistance for both stamped and hydroformed plates when compared with non-deformed blank plates of SS304. In addition, it was observed that there exist an optimal process window for punch speed in stamping and the pressure rate in hydroforming to achieve improved corrosion resistance at a faster production rate.

1. Introduction

Fuel cell technologies enable clean energy generation, zero-emissions, and reduction of greenhouse gas emissions. Polymer electrolyte membrane, also known as proton exchange membrane fuel cells (PEMFCs) have emerged as the leading candidates to replace internal combustion engines (ICEs) in vehicles and provide compact portable energy to other small-scale devices. Unfortunately, PEMFCs have not been commercialized in full scale yet, mainly due to issues related to their high cost, low durability and reliability. The main components of the PEMFC stack are the membrane, the catalyst layer, and the bipolar plate. These components also constitute the majority of the fuel cell cost. Among these components, however, bipolar plates stand as the high weight-, high volume-, and high cost-component (i.e., 60–80% of stack weight, 30–45% of stack cost) [1,2]. In the past few years, the fabrication methods and material selection for bipolar plates in PEMFCs for vehicle applications have gradually evolved and narrowed to the following few candidates: (1) machined graphite plates, (2) stamped or photo etched metal plates with and without coatings, (3) molded polymer-carbon composite, and (4) molded carbon–carbon material [3]. Metallic bipolar plates have several advantages over other types of bipolar plates (e.g., graphite and composite) as a fuel cell stack component for mass production purposes due to their high conductivity, low material and production costs, and the ability of achieving thinner plates. The graphite bipolar plates have been used for a long time in lab-scale demonstrations, but are not considered for mass-scale applications due to the high cost of machining needed to manufacture micro-channels on the surface and the brittleness that leads to durability problems. Metallic bipolar plates are expected to overcome the cost and durability issues that the graphite bipolar plates have.

Metallic bipolar plates can be manufactured by various methods including machining, stamping, die casting, investment casting, powder metal forging, electroforming, stretch forming, wire bonding, and hydroforming [4]. Among these, stamping and hydroforming are seen as the suitable approaches for mass production scales. For instance, for a production plan of 100,000 cars per year, 40 millions bipolar plates of around 30 cm × 30 cm must be manufactured to the very tight specifications at a rate of approximately two plates per second. Both stamping and hydroforming processes can potentially achieve this production rate. Other pro-

* Corresponding author at: Virginia Commonwealth University, Mechanical Engineering, 601 W Main St., PO Box 843015, Richmond, VA 23284, USA.
Tel.: +1 804 827 7029; fax: +1 804 827 7030.
E-mail address: mkoc@vcu.edu (M. Koç).

0378-7753/$ – see front matter © 2010 Elsevier B.V. All rights reserved.
doi:10.1016/j.jpowsour.2009.12.040

duction methods can hardly reach such production rates. The outstanding advantage of the stamping comes from the fact that it is fast and inexpensive, while that of the hydroforming comes from good surface topology, uniform thickness distributions, and tight dimensional tolerances that would potentially help maintaining a desirable fuel cell performance.

The selection of manufacturing process will have major effects on the dimensional and surface properties of the bipolar plates. After a flat metal sheet is shaped into arrays of micro-channels (i.e., flow field), the surface becomes harder, the thickness distribution changes, the surface roughness varies, the coating layer is deformed and fractured, and there will be some residual stress left on the metal sheet. These changes eventually affect the corrosion, the contact mechanics; and hence, the performance of the fuel cell. Metallic plates with appropriate coatings may have a good corrosion resistance before manufacturing (shaping), but they are susceptible to increased corrosion after deformation due to the local loss of coating layer by scratching or galling typically observed in stamping process. There are various existing publications discussing the corrosion and contact mechanics properties of different flat metal sheets [5–8]; however, there is no study acknowledging the very same issues for manufactured or shaped bipolar plates with flow field. The effects of stamping and hydroforming of thin metal sheets on the corrosion resistance is the main focus of this study.

2. Review of corrosion resistance issues in PEMFC bipolar plates

Corrosion resistance of a material is the resistance to the dissolution of the material from the surface. The rate of dissolution or corrosion rate depends on the cell environment (e.g., temperature, applied potential, electrolyte), type of material (steady state potential, material passivity, the surface affinity), and the surface quality. The corrosion potential shows the corrosion resistance of the material according to thermodynamic laws, whereas the corrosion current shows the corrosion resistance of the material according to kinetic laws [9].

In PEMFC applications, corrosion of metallic bipolar plates is one of the most researched issues. As the metallic bipolar plates corrode, metal ions are released and block the ion conduction mechanism for H^+ at the membrane [10]. Also, the contact resistance will increase due to the oxide layer formation at the surfaces [11]. Eventually, the corrosion of the metallic bipolar plates would directly lead to performance degradation and a shorter stack life.

The United States Department of Energy (DOE) has put certain goals for metallic bipolar plates to be used in fuel cell stacks. The corrosion goals by the year 2010 are set as follows. At the anode side, the corrosion current at 0.1 V vs. SHE (standard hydrogen electrode) while hydrogen is bubbling through an acid solution (representing the acidic fuel cell environment) should not exceed 1 $\mu A\,cm^{-2}$ [12,13]. On the other hand, at the cathode side, the corrosion current at 0.85 V vs. SHE while oxygen is bubbling through an acid solution should also not exceed 1 $\mu A\,cm^{-2}$. In addition, the contact resistance and cost of a metallic bipolar plate are aimed to be less than 10 $m\Omega\,m^2$ at 140 $N\,mm^{-2}$ and \$6 kW^{-1}, respectively [12,13].

Even though different commercially available stainless steel grades possess a relatively good corrosion resistance, most of them still could not survive in the acidic environment of PEMFCs to meet the DOE goals without appropriate surface modification (i.e., coating) [5–7]. The corrosion current values for such steel grades are reported to be between 8 and 52 $\mu A\,cm^{-2}$ as summarized in Table 1. In order to meet the goals for corrosion resistance, they must be coated with a better corrosion resistant material. Several coatings on commercial materials have been tested to accomplish the DOE targets set for corrosion resistance [7,10,14,15]. While some of the coating materials enhanced the corrosion resistance and met the DOE target (<1 $\mu A\,cm^{-2}$), they failed to meet the contact resistance goal (<10 $m\Omega\,m^2$ at 140 $N\,mm^{-2}$). Yoon et al. showed that a gold coating could significantly decrease the contact resistance. In addition, they reported that a 10 nm thick coating on several types of base materials would be enough to meet the DOE goals [14]. Table 2 summarizes a list of the corrosion and contact resistance of some coated metals.

Therefore, it is essential to coat or modify the surface of the stainless steel plate in order to meet the DOE targets. The most commonly used coating materials are either carbon based or metal based. Graphite, conductive polymers, diamond like carbon and organic self-assembled polymers are examples of carbon-based coating, whereas metal-based coating materials are usually noble metals, such as metal nitrides and metal carbides [4]. The coating thickness is another important parameter that determines the corrosion resistance, contact resistance, and the overall cost [14].

Coating can be applied before or after the manufacturing process of the micro-channels (i.e., flow field) on the plates. There are many studies investigating different coatings and surface modification of stainless steel sheets, but all of them, so far, focused on non-deformed stainless steel sheets (i.e., flat sheets). The effect of manufacturing process on the corrosion and contact mechanics of the uncoated, coated and modified plates have not yet been investigated and reported in any open literature. Such lack of knowledge in the effect of manufacturing on corrosion resistance has inspired and set a scope for this study, in which only uncoated metallic plates were stamped and hydroformed under different processing conditions for corrosion testing. Coated metallic plates will be investigated in a follow up study.

3. Manufacturing of thin metallic bipolar plates

For this study, stamping and hydroforming were selected to fabricate micro-channel arrays on thin sheets of SS304 with an initial thickness of 51 μm. While stamping required both male and female dies for forming the channels, hydroforming process required only the female die with pressurized fluid as the forming media (Figs. 1 and 2). The most outstanding known advantage of stamping process is its fast cycle time, while that of hydroforming process is the uniform dimension and thickness distribution on the micro-channel arrays. Even though different types of stainless steels (e.g., SS304, SS316, SS316L, SS317L, SS904L, SS349, Krofer, Nikrofer) could be used as a base material for bipolar plates, SS304 was selected in this study for its low material cost, acceptable corrosion resistance and availability.

In a previous study, the effects of process conditions (e.g., stamping force and speed, and hydroforming pressure and pressure rate) on the manufacturability of the bipolar plates were investigated in detail [16]. In summary, it was reported that the micro-channel depth (or height) increases with increasing stamping force or hydroforming pressure. In addition, hydroforming was found to provide low dimensional variation on the micro-channel arrays when compared to the stamping process. The effects of the stamping speed (between 0.1 and 1 $mm\,s^{-1}$) and the hydroforming pressure rate (at 0.1, 1, and 10 $MPa\,s^{-1}$) were also found to be significant on the formability of the micro-channels, especially at a lower stamping force level.

4. Corrosion resistance tests of thin metallic bipolar plates

It is hypothesized that the manufacturing of bipolar plates affects the corrosion resistance mainly due to altered surface topog-

Table 1
Corrosion current in 0.5 M H_2SO_4 media and contact resistance values for bare stainless steels.

Stainless steel material	i_{corra} at 0.1 V ($\mu A\,cm^{-2}$)	i_{corrc} at 0.85 V ($\mu A\,cm^{-2}$)	R_{ct} ($m\Omega\,cm^2$)	Refs.
304	35[a]	35[a]	~75	[12,18]
316	–	–	~100	[11]
316L	~52	~14	~150	[10]
317L	~21	~17	~148	[10]
904L	~16	~9.5	~132	[10]
349	~9.5	~11	~112	[10]
AISI 444	~50	~20	~100	[19]
AISI 446	~8	~20	~200	[19]

[a] These values were recorded without purging any gas.

Table 2
Corrosion current in 0.5 M H_2SO_4 media and contact resistance values for coated metal plates.

Base material	Coating material	i_{corra} at 0.1 V at 80 °C ($\mu A\,cm^{-2}$)	i_{corrc} at 0.85 V at 80 °C ($\mu A\,cm^{-2}$)	R_{ct} ($m\Omega\,cm^2$)	Refs.
SS316	TiN	~0.2 (0 V)	~0	–	[13]
AISI 446	Nitrided	~0.2–1.7	~0.6–1.5	~6–40	[6]
SS316	Carburized	~7	~1.5	~75	[12]
SS316	Zr	~0.15	~0.35	~1000	[14]
SS316	ZrN	~0.2	~4	~160	[14]
SS316	ZrNAu	~2.5	~1.5	~6	[14]
SS316	Au	~4	~4	~5	[14]

raphy, and possibly the residual stresses, after plastic deformation of the thin metallic blank into micro-channel array. In order to quantitatively reveal the effect of manufacturing on corrosion resistance, both non-deformed (i.e., incoming flat blank) and deformed (i.e., stamped and hydroformed plates) SS304 plates were tested for their corrosion resistance properties as explained in the following sections.

4.1. Corrosion resistance test methods

Electrochemical methods such as potentiodynamic and potentiostatic measurements are the most commonly used methods to observe the corrosion behavior of metallic bipolar plates [13,15]. Surface analysis such as microscopy (light, SEM) and other instrumental methods (EDX, XRAY, XPS) can also be used. Corrosion resistance can also be measured by the amount of ions released from metallic plates.

The corrosion potential of a substrate can be obtained from the open circuit potential of the metal substrate in liquid electrolyte. In order to observe the behavior of the electrode in varying potentials, a potentiodynamic experiment should be conducted. This experiment indicates whether the electrode is in an active or passive state for corrosion as well as providing initial corrosion current values at certain potentials regardless of time [9]. A linear sweep voltammetry experiment can be conducted between an anodic corroding potential and a cathodic corroding potential. The transition from the anodic polarization to the cathodic polarization represents the corrosion potential value. The corrosion current can be

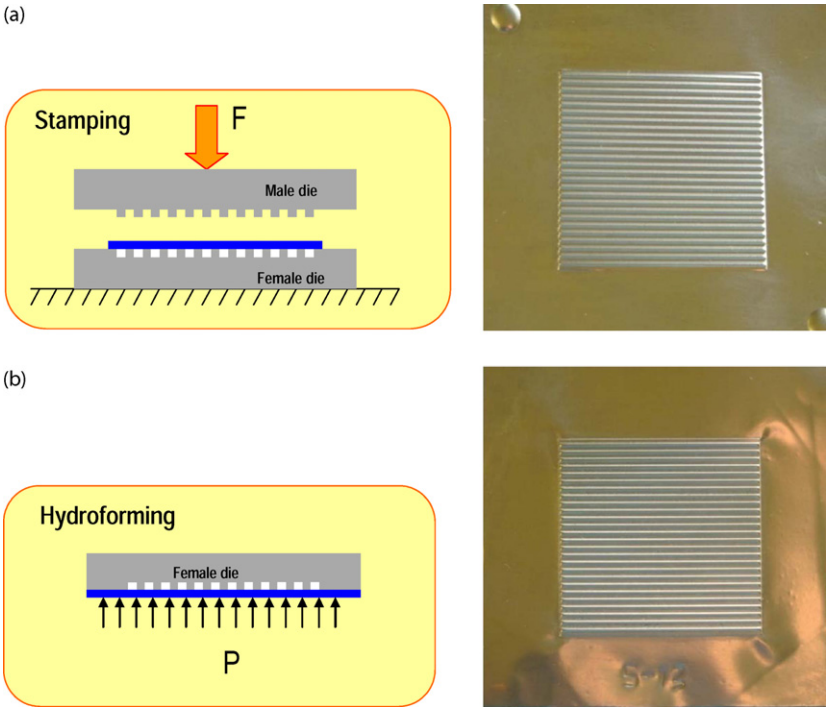

Fig. 1. Schematic diagram and samples from (a) stamping, and (b) hydroforming processes.

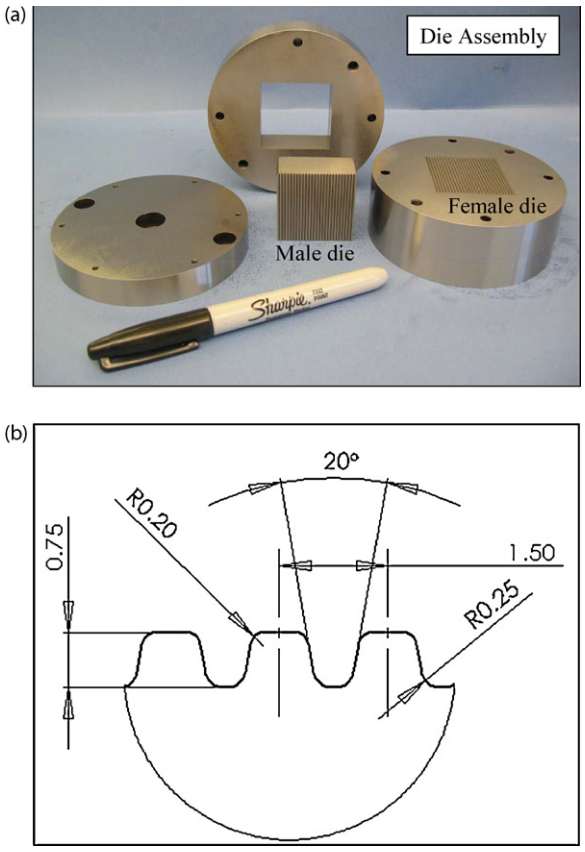

Fig. 2. (a) Die set for stamping and hydroforming and (b) detail geometry of microchannel on the female die (units are in mm).

obtained from the intersection of the tangential lines to the negative and positive overpotential curves as explained elsewhere [9].

In this study, a custom made corrosion cell controlled with a PAR 2200 potentiostat (Fig. 3) was used to carry out both potentiodynamic and potentiostatic experiments on initial flat blanks (non-deformed), stamped, and hydroformed bipolar plates. The corrosion cell consists of a specimen holder where a metal blank (bipolar plate) is held inside and acts as a working electrode, a Poco graphite counter electrode, an Ag/AgCl reference electrode, and a gas bubbler at the bottom. To simulate the PEMFC environment, 0.5 M H_2SO_4 solution was used as the working electrolyte while the temperature of the corrosion cell was controlled at 80 °C by an electrical furnace.

The specimen preparation steps are as follows: first, the residual oil and dirt on the specimen surface were removed by wiping with acetone, followed by ultrasonic cleaning for 30 min in an acetone bath. Next, the non-active area and the back part of the bipolar plate specimens were covered with a chemically stable and insulator Teflon tapes; and thus, only the active area of the bipolar plate was exposed to the acid. The working electrode (i.e., bipolar plate) was placed in the corrosion cell before placing the electrolyte. All connections inside and around the cell were covered with Teflon tape to prevent the corrosion from the sulfuric acid vapor. Additional 0.5 M H_2SO_4 was also placed inside the temperature controlled environment with a closed tap to prevent excessive evaporation of the acid at 80 °C. The acid was refilled several times during the experiment to ensure that the working electrode is fully submerged under the electrolyte throughout the entire test period.

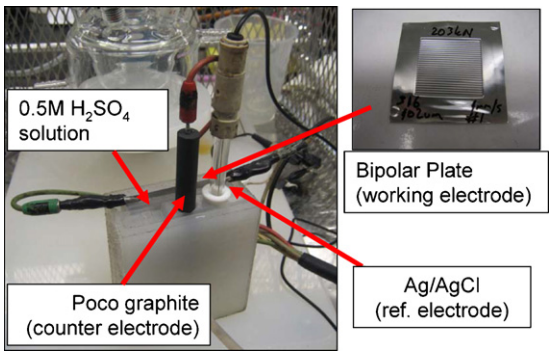

Fig. 3. Corrosion test setup.

The potentiodynamic experiments were performed by increasing the potential from −1.0 to 1.0 V at a rate of 1 mV s^{-1}, as also selected in similar studies [14,17]. All of the potentials were given with respect to the standard hydrogen electrode. The upper and lower limits of the experiment were selected to include the anodic and cathodic transition potentials with an adequate offset for extrapolation. Three different potentiodynamic conditions were carried out which include: no gas (acidic condition), H_2 purge (anode side condition), and O_2 purge (cathode side condition). The graphs were plotted between −0.6 and 1 V for improved visibility. On the other hand, the potentiostatic experiments represent the steady state operation condition of the fuel cell where the current values were obtained and recorded when the system reached the steady state while keeping the potential constant at 0.8 V vs. SHE during O_2 purge and at 0.1 V during the H_2 purge [13].

4.2. Potentiodynamic test results

4.2.1. Interpretation of result and repeatability

At the early stages of the study, a number of experiments were conducted to ensure good repeatability of the test setup. As illustrated in Fig. 4, the tangential line of the anodic polarization curve was drawn to determine the corrosion current values [9] since the cathodic polarization curve was not suitable for extrapolating a tangential line due to two different oxidation processes had occurred in the potential range between −0.2 and −0.4 V (first peak or half peak from the bottom). The duration of the oxidation process was around 3–5 min while the potential continued to shift. The breakdown of the surface oxide due to the plastic deformation during the rolling process to produce the thin sheet, the stamping and

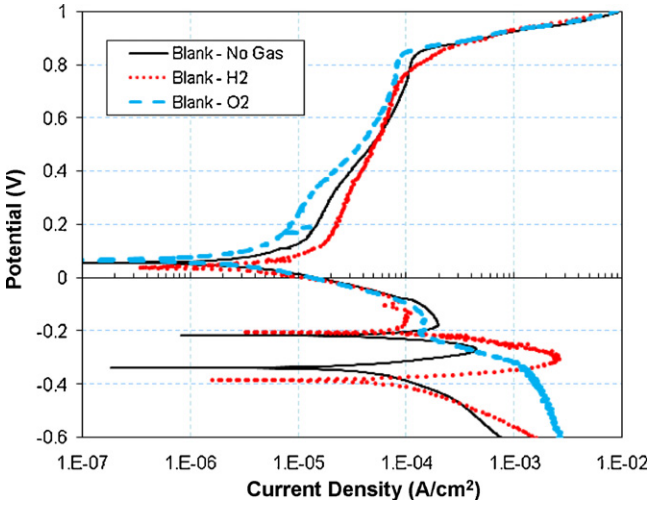

Fig. 4. The effect of purged gases on corrosion resistance of non-deformed SS304 blanks.

hydroforming processes to produce the micro-channels; and the re-oxidation of the bulk material's surface could be the reasons for the early peaks. The second peak as shown in Fig. 4 indicates the point where the oxidation of these areas was completed, while the third peak represents the transition point between reduction and oxidation regions. Among these peaks, the third peak was chosen for comparison since the region between the first two peaks was briefly interrupted and unstable. In addition, the occurrence of all three peaks was independent from one another; and thus, the first two peaks did not have any effect on the third peak. On the other hand, the surface oxidized very quickly on the cathode side; and thus, the second and third peaks were not observed in the case of O_2 purging experiments. This might be due to the early oxidation of the cracked areas before the potentiodynamic experiment process started.

4.2.2. Effect of purging gases on corrosion resistance

The hydrogen and oxygen gases were purged during the potentiodynamic experiments for the non-deformed SS304 samples (Fig. 4) to resemble the corrosive environment inside a fuel cell stack. Based on the results in Fig. 4, the presence of hydrogen and oxygen gases are shown to have an effect on the corrosion resistance of the plate. Specifically, hydrogen has a significant negative effect on the corrosion resistance, whereas the corrosion resistance is shown to improve in the presence of oxygen.

4.2.3. Effect of fabrication process on corrosion resistance

For reasonable comparisons between the two forming processes, the ranges of the stamping force and hydroforming pressure were selected to be between 100–300 kN and 20–60 MPa, respectively. This way, for a given plate size of 70 mm × 70 mm, the stamping force would be in a similar range with the hydroforming pressure [16]. In addition, the effect of the stamping speed (0.1–1 mm s^{-1}) and hydroforming pressure rate (0.1–10 MPa s^{-1}) on the corrosion resistance was also considered.

As expected, the corrosion current was shown to increase (lower corrosion resistance) with increasing stamping force as shown in Fig. 5a. On the other hand, only a slight effect of the hydroforming process could be observed on the corrosion resistance since there was no significant difference in potentiodynamic results between the hydroformed and non-deformed plates (Fig. 5b). When examined closely, the surface topologies of the hydroformed plates were found to be improved due to the surface smoothing under uniform and homogeneous pressure distribution during the hydroforming process as shown in Fig. 6b as compared to Fig. 6a. The small improvement in surface quality of stamped specimen (Fig. 6c) can be attributed to the surface smoothening by stretching. Furthermore, the surface topography of the blank, stamped and hydroformed specimens were examined with an optical 3D measurement system (Nanofocus, μSurf Explorer) as shown in Fig. 7. Notice that the rolling marks can be clearly seen on the non-deformed blank as illustrated in Fig. 7a. The measurement of the surface roughness value (R_a) was performed on both non-deformed and deformed specimens. The R_a values of non-deformed, hydroformed at 40 MPa, 1 MPa s^{-1} (Fig. 7b) and stamped at 200 kN, 1 mm s^{-1} (Fig. 7c) plates were found to be 0.060, 0.050 and 0.055 μm, respectively. These R_a values represent the average roughness value of the selected section on the plate (i.e., localized data); and thus, could not be directly used to reflect on the corrosion resistance.

The results from the potentiodynamic tests for all cases are summarized in Fig. 8. The test results with purging H_2 gas (Fig. 8a) indicate that the corrosion resistance of the non-deformed plate was better than the hydroformed plates, except for one extreme case (i.e., hydroformed 60 MPa), but worse than stamped plates,

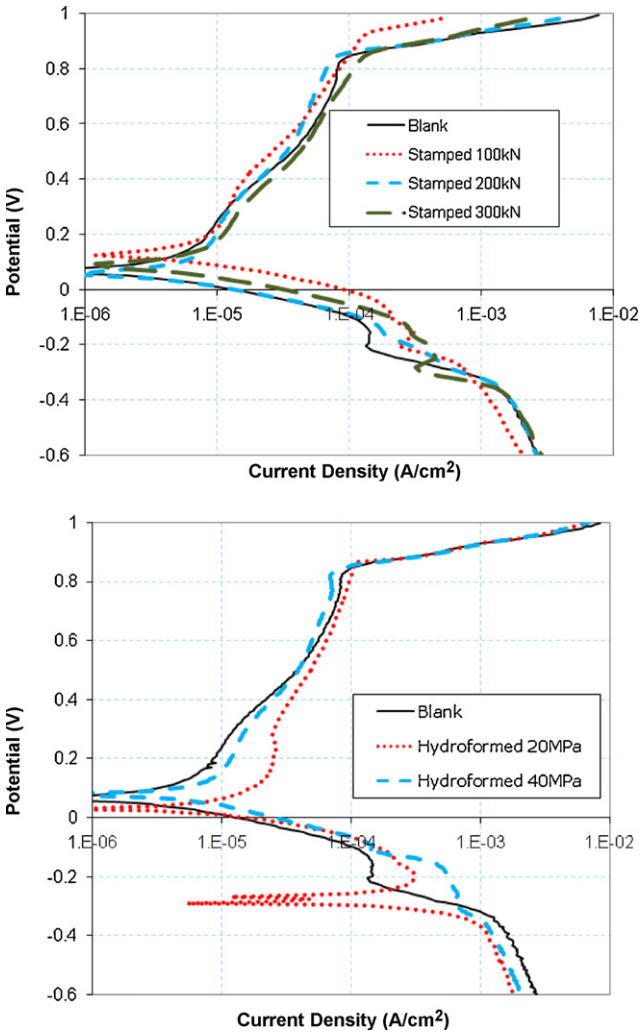

Fig. 5. Effect of stamping force and hydroforming on corrosion resistance during H_2 purging.

except for one extreme case (i.e., stamped 300 kN). In other words, the high pressure level smoothened the surface of the hydroformed plates, while the high stamping force generated scratches on the surface of the stamped plates.

Corrosion resistance results with purging O_2 gas were slightly different from with purging H_2 gas as shown in Fig. 8b. In general, the non-deformed plate showed better corrosion resistance when compared to the hydroformed and stamped plates. The corrosion resistance values of stamped plates at different force levels were found to be very similar and are slightly better than that of the hydroformed plates.

The effects of the punch speed and pressure rate on the corrosion performance are shown in Fig. 8a and b, respectively. The results show that a faster stamping speed (1 mm s^{-1}) resulted in bipolar plates with better corrosion resistance when compared to a slower stamping speed (0.1 mm s^{-1}) in the presence of either H_2 or O_2 gases. Therefore, a 1 mm s^{-1} should be selected over 0.1 mm s^{-1} during the stamping process due to better corrosion resistance and faster cycle time. Finally, the corrosion resistance was found to improve when a slower pressure rate was used during the hydroforming process under both anodic and cathodic environments. However, this improvement in corrosion resistance will come at a cost of a longer process cycle time; and therefore, an optimum pressure rate would need to be determined.

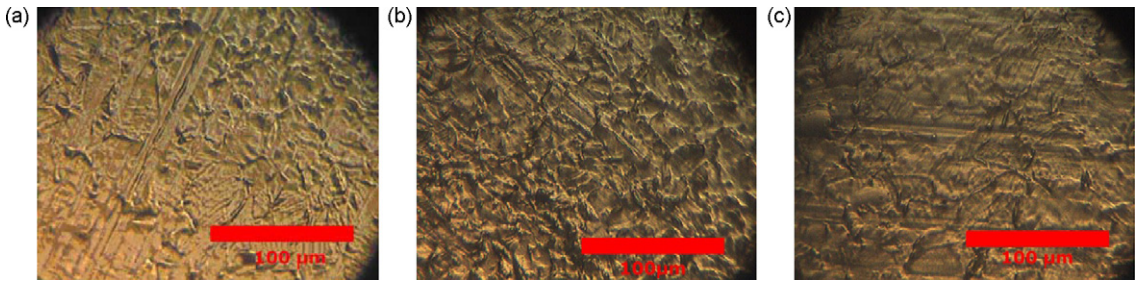

Fig. 6. Surface topology of (a) non-deformed, (b) hydroformed, and (c) stamped SS304 plates.

4.3. Potentiostatic test results

The potentiostatic experiment results showed an increase in corrosion current under H_2 purging condition before the value decreased and become stabilized (Fig. 9a). On the other hand, in the case of O_2 purging, the corrosion current was found to continuously decrease until it became stabilized (Fig. 9b). The stabilization time period was found to vary according to the surface homogeneity of the specimens. Nonetheless, hydroformed specimen surfaces appeared to be more homogenized than stamped specimen surfaces due to a shorter stabilization time. The test results under H_2 purged condition showed poorer corrosion resistance of both non-deformed and deformed plates when compared to the O_2 purged condition; and thus, the anodic side can be said to be more corrosive than the cathodic side. Finally, the drop in corrosion resistance with stamped and hydroformed samples can be clearly observed when compared to the non-deformed (blank) samples in the case of O_2 purged condition. However, comparing between the two manufacturing processes, the hydroformed plates showed more resistance

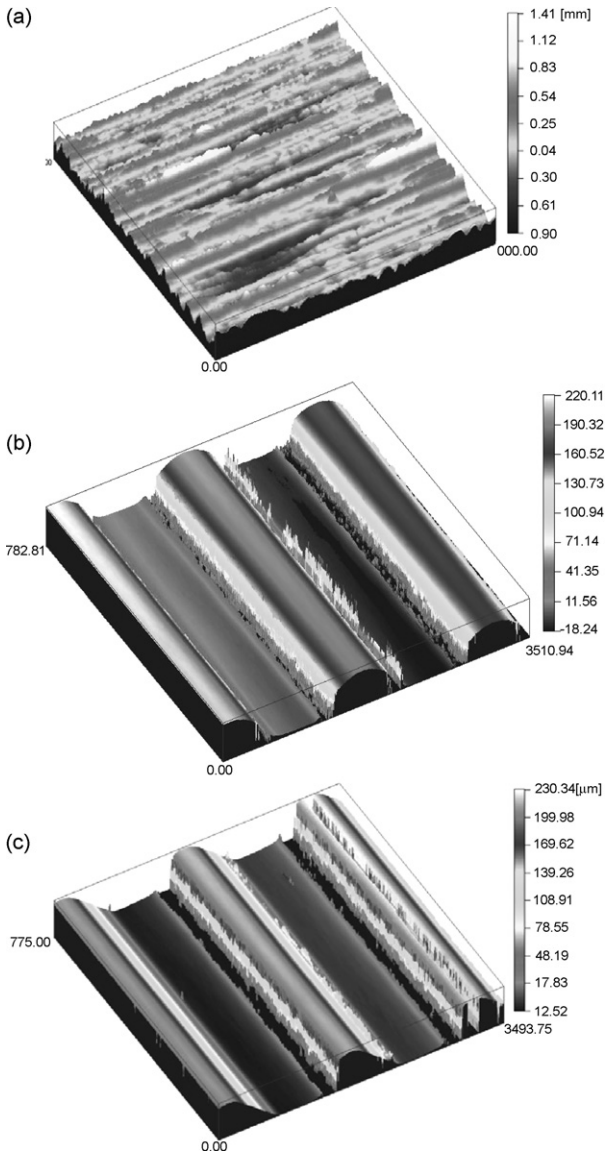

Fig. 7. Surface Roughness of (a) non-deformed, (b) hydroformed, and (c) stamped SS304 plates.

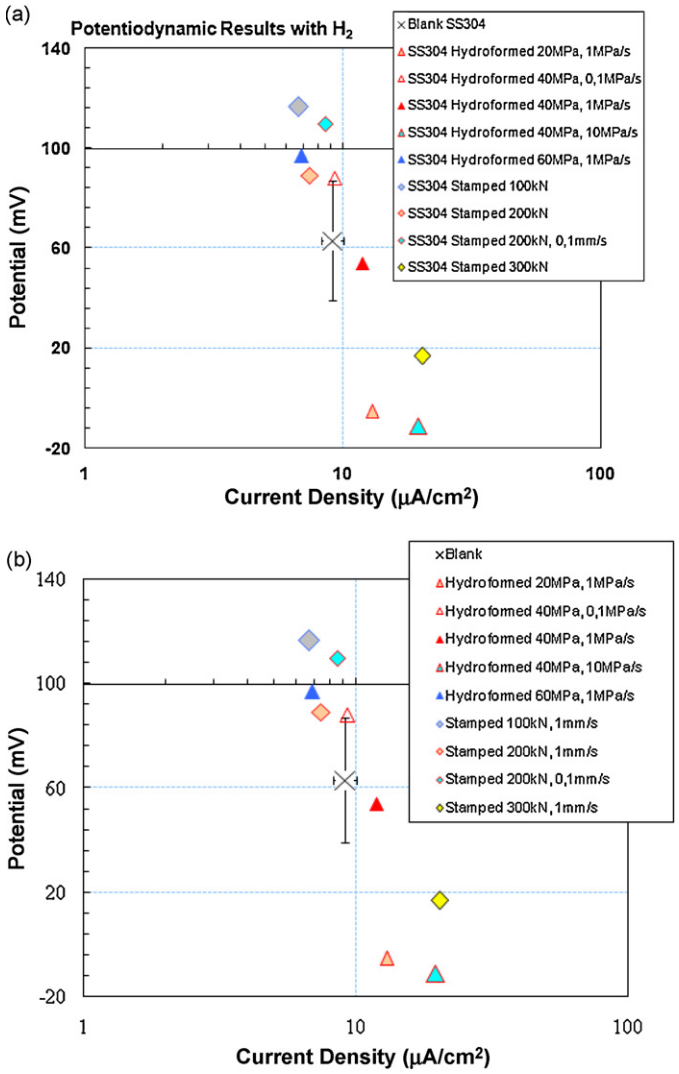

Fig. 8. Effect of pressure and stamping force on corrosion resistance with purging: (a) H_2 gas and (b) O_2 gas.

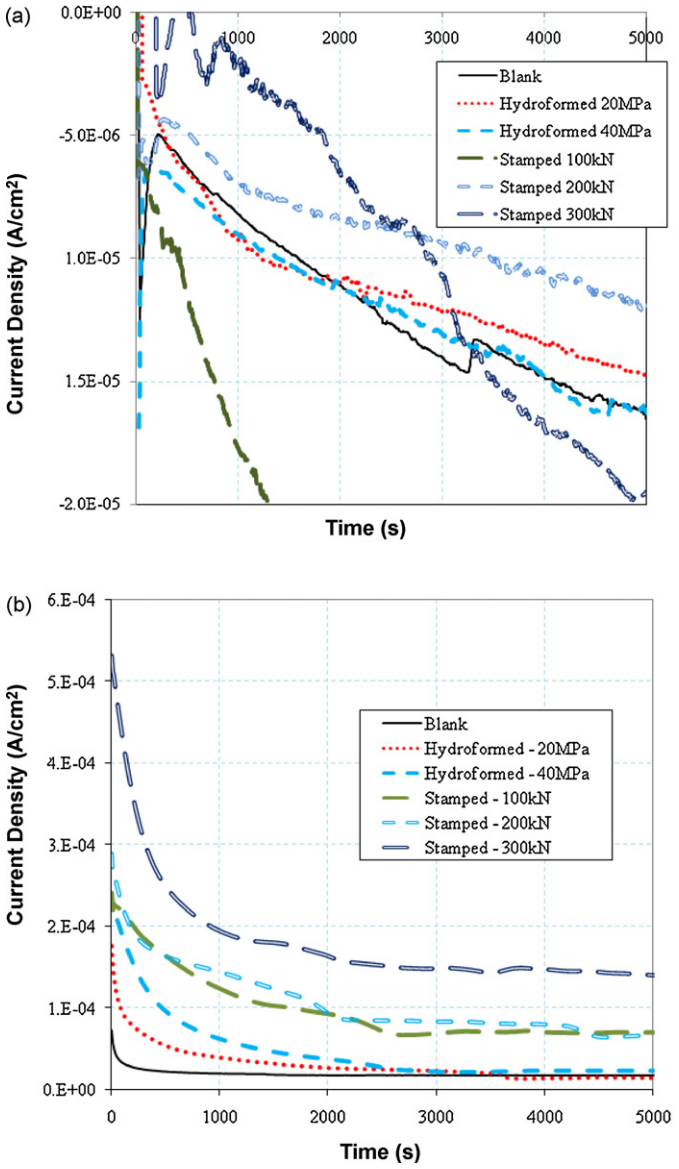

Fig. 9. Potentiostatic corrosion resistance of non-deformed, stamped and hydroformed samples with purging: (a) H_2 gas and (b) O_2 gas.

to the corrosive environment in the fuel cell stacks when compared to the stamped plates.

5. Summary and conclusions

In this study, the effects of manufacturing processes (i.e., stamping and hydroforming) and process conditions on the corrosion resistance of thin metallic bipolar plates were investigated. The results showed that the manufacturing processes would generally degrade the corrosion resistance when compared to non-deformed blanks. Although this observation held true for most of the cases, in a few instances, especially during potentiodynamic experiments, the opposite trend was also observed. This can be explained with the removal of residual stresses which occurred after several plastic deformation processes and smoothening of the surfaces. The metallic bipolar plates need to be corrosion resistant under both anodic and cathodic conditions; the results showed that a much improvement of the surface quality is needed, especially under the anodic condition.

The effect of process conditions in both stamping (punch speed) and hydroforming (pressure rate) was shown to be significant on the corrosion performance of the plates. Specifically, lower stamping speed resulted in more surface scratches and damages, which in turn, gave rise to decreased corrosion resistance. Therefore, based on the results in this study, a faster stamping speed should be selected for the fabrication of bipolar plates since it resulted in better corrosion resistance and also a shorter production time. On the other hand, the lower pressure rates in hydroforming were shown to result in an increase in corrosion resistance. Unfortunately, the pressure rate needs to be high for mass production requirement. Therefore, a compromise between corrosion performance and production rate is needed if hydroforming will be selected for a mass production of the metallic bipolar plates.

As a final remark, surface coating is necessary in order to enhance the corrosion properties of the bipolar plate to meet the DOE goals. In the near future, the effects of different coating materials, coating techniques, and the sequence of the coating process (i.e., coating before or after forming process) on the corrosion resistance as well as the contact mechanics of the metallic bipolar plates will be investigated.

Acknowledgments

Authors are thankful to National Science Foundation (NSF) for the support on this project. It was supported by NSF I/UCRC Program (Center for Precision Forming-CPF and its industrial members under NSF IIP Grant #: 0638588). The authors also would like to thank Hamilton Precision Metals, Inc. for the supply of sheet materials and their properties.

References

[1] A. Hermann, T. Chaudhuri, P. Spagnol, International Journal of Hydrogen Energy 30 (2005) 1297–1302.
[2] X. Li, I. Sabir, International Journal of Hydrogen Energy 30 (2005) 359–371.
[3] M. Koç, S. Mahabunphachai, Journal of Power Sources 172 (2) (2007) 725–733.
[4] V. Mehta, J.S. Cooper, Journal of Power Sources 114 (2003) 47.
[5] H. Wang, M.A. Sweikart, J.A. Turner, Journal of Power Sources 115 (2003) 243–251.
[6] T. Fukutsuka, T. Yamaguchi, S. Miyano, Y. Matsuo, Y. Sugie, Z. Ogumi, Journal of Power Sources 174 (2007) 199–205.
[7] V.V. Nikam, R.G. Reddy, S.R. Collins, P.C. Williams, G.H. Schiroky, G.W. Henrich, Electrochimica Acta 53 (2008) 2743–2750.
[8] H. Wang, J.A. Turner, Journal of Power Sources 128 (2004) 193–200.
[9] D.A. Jones, Principles and Prevention of Corrosion, Prentice–Hall Inc., 1996, pp. 8, 77–90.
[10] H. Tawfik, Y. Hung, D. Mahajan, Journal of Power Sources 163 (2007) 763–767.
[11] R.F. Silva, A. Pozio, Journal of Fuel Cell science and Technology 4 (2007) 116–122.
[12] DOE Website, http://www1.eere.energy.gov/hydrogenandfuelcells/mypp/, 2009, Section 3.4, p. 26.
[13] J.A. Turner, Wang, H., DOE Annual Progress Report, 2005.
[14] M. Li, S. Luo, C. Zeng, J. Shen, H. Lin, C. Cao, Corrosion Science 46 (2004) 1369–1380.
[15] W. Yoon, X. Huang, P. Fazzino, K.L. Reifsneider, M.A. Akkaoui, Journal of Power Sources 179 (2008) 265–273.
[16] S. Mahabunphachai, M. Koç, Proceedings of the International Conference on Multi-Material Micro-Manufacture(4M) and International Conference on Micro-Manufacture (ICOMM), September 23–25, Forschungszentrum Karlsruhe, Germany, 2009.
[17] M.A. Lucio Garcia, M.A. Smit, Journal of Power Sources 158 (2006) 399.
[18] J. Jagielski, A.S. Khanna, J. Kucinski, D.S. Mishra, P. Racolta, P. Sioshansi, E. Tobin, J. Thereska, V. Uglov, T. Vilaithong, J. Viviente, S. Yang, A. Zalar, Applied Surface Science 156 (2000) 63.
[19] Y. Wang, D.O. Northwood, Electrochimica Acta 52 (2007) 6793–6798.